Original Research Article

Heat and Mass Transfer of a Chemically Reacting MHD Micropolar Fluid Flow over an Exponential Stretching Sheet with Slip Effects

Abstract
This work investigates flow, heat and mass transfer of a chemically reacting and electrically conducting micropolar fluid over an exponentially stretching sheet in the presence of thermal radiation, viscous dissipation, suction/injection, heat source/sink and slip effects. The system of the governing partial differential equations of the fluid flow is transformed into nonlinear ordinary differential equations by applying similarity variables. The resulting equations are numerically solved by shooting method alongside fourth order Runge-Kutta integration technique. The influences of the controlling flow parameters on the dimensionless velocity, angular velocity, temperature and species concentration profiles as well as on the skin friction coefficient, wall couple stress, heat and mass transfer rates are presented through graphs and tables. Comparison of the present results with previously published work in the literature for some limiting cases shows a good agreement.
Keywords: Micropolar fluid; exponential stretching; slip effects; suction/injection

1 Introduction

In the recent times, engineers and researchers have developed interest in the study of non-Newtonian fluids due to the increasing practical usefulness and relevance of these fluids in many industrial and technological processes like polymer engineering, crude oil extraction, food processing manufacturing and many others. Among the various non-Newtonian fluids models, the micropolar fluids theory developed by Eringen [1] and extended to thermo-micropolar fluids also by Eringen [2] has gained prominence. This because the theory of micropolar fluids provides a good mathematical model for investigating the flow of complex and complicated fluids such as suspension solution, animal blood, liquid crystals, polymeric fluids and clouds with dust [3-4].

Micropolar fluids are fluids with microstructure which belong to the class of fluids that exhibit certain microscopic effect arising from the local structure and micromotion of the fluid element. Physically, micropolar fluids may represent fluids consisting of rigid, randomly oriented (or spherical) particles suspended in a viscous medium, where particles deformation is ignored, they also belong to the group of fluids with non-symmetric stress tensor that are called polar fluids which constitute a substantial generalization of the Navier-Stokes model. Such fluids are of a complex nature and individual fluid particles may be of different shapes and may shrink and/or expand, occasionally changing shapes and rotating independently of the rotational movement of the fluid Lukaszewicz [5]. Peddieson and McNitt [6] first studied the boundary layer flow of such fluids, thereafter, several authors have investigated these fluids on different geometries and conditions.

The boundary layer flow past stretching sheet is significant in engineering processes such as extrusion of plastic sheet, glass blowing, hot rolling, textile and paper production. Pioneering the work on boundary layer flow induced by stretching sheet, Crane [7] investigated linearly stretching sheet on the steady two-dimensional problem and gave the similarity solution in closed analytical form, Gupta & Gupta [8] extended the work of Crane to include heat and mass transfer on stretching sheet with suction or blowing. Eldabe *et al.*, [9] studied MHD flow of a micropolar fluid past a stretching sheet with heat transfer. Elbashbeshy and Bazid [10] examined heat transfer over a stretching sheet embedded in a porous medium. Recently, Reddy [11] examined heat generation and thermal radiation effects over a stretching sheet in a micropolar fluid.

In some practical situations, however, the stretching of plastic sheet may not necessarily be linear, it may be nonlinear and/or the exponential type. The flow, heat and mass transfer characteristics over an exponentially stretching sheet has numerous applications in technology such as in the case of annealing and thinning of copper wire. In such cases, the end product depends on the rate of heat transfer at the stretching continuous surface with exponential variations of stretching velocity and temperature distribution (Mukhopadhyay [12]). However, a little attention has been paid to the study of flow over an exponentially stretching sheet in spite of its important applications in many engineering operations. Pioneering the flow over an exponentially stretching sheet, Magayari and Keller [13] studied heat and mass transfer on boundary layer flow induced an exponentially stretching sheet with exponential temperature distribution. Later, Sajid and Hayat [14] considered the influence of thermal radiation on the boundary layer flow due to exponentially stretching sheet. El-Aziz [15] extended the work of Magayari and Keller [13] by investigating viscous dissipation effect on mixed convection flow of a micropolar fluid over an exponentially stretching sheet. Mandal and Mukhopadhyay [16] investigated heat transfer analysis for fluid flow over an exponentially stretching porous sheet with surface heat flux. Recently, Seini and Makinde [17] examined MHD boundary layer flow of a Newtonian fluid due to exponential stretching surface with radiation and chemical reaction.

The boundary layer flow, heat and mass transfer of an electrically conducting fluid over stretching surfaces has important applications in manufacturing and engineering processes such as hot rolling, wire drawing, the extrusion of polymer sheet from a die and the cooling of metallic sheets. In such processes, the quality of the final product depend to some extent on the kinematics of stretching and the simultaneous rate of heating and cooling during the fabrication processes. Thus, the rate of cooling can be controlled by the use of electrically conducting fluid and that of magnetic field. Kumar [18] numerically studied the problem of heat and mass transfer in a hydromagnetic flow of a micropolar fluid past a stretching sheet using the Finite element technique. It was reported that the fluid velocity increased with a rise in the material parameter while the opposite was the case with increase in the magnetic field parameter. Similarly, microrotation, concentration and temperature were increasing functions of magnetic field parameter.

Many of the engineering and manufacturing operations occur at high temperature, thus, the effect of thermal radiation on magnetohydrodynamic flow, heat and mass transfer becomes very important for the design of relevant equipment such as the design of fins, steel rolling, nuclear power plants, electric power generation and solar power technology. Due to this many researchers have reported the influence of thermal radiation on fluid flow (Ibrahim [19]; Hamad *et al.* [20]]).

The study of boundary layer flow involving chemical reaction and heat generation/absorption has drawn the attention of many researchers due to its important applications in many engineering processes such as in chemical processes and hydrometallurgical industries, for example, food processing, smog formation, groves of fruit trees and crop damage due to freezing and manufacturing of ceramics and polymer production (Das[21]; Mishra *et al.* [22]). Likewise, heat generation/absorption effect may change the temperature distribution of the fluid flow and in consequence affect various engineering devices. Such study has attracted researchers such as (Ibrahim, [18]; (Olajuwon *et al.* [23]; Pal and Chatterjee [24]).

Many of the researchers above have investigated the flow and heat transfer problems of Newtonian/non-Newtonian fluids with the assumption of no-slip boundary condition which is the central tenet of the Navier-Stokes theory. However, it has been observed that the assumption of no-slip boundary condition does not hold in some practical situations and hence, it may be necessary to replace the no-slip boundary condition with the partial slip boundary conditions. The non-adherence of fluid to a solid boundary is known as velocity slip. The slip and temperature jump boundary conditions represent a discontinuity in the transport variable across the interface and describes more accurately the non-equilibrium region near the surface. Slip flow problems are important when considering particulate fluids e.g. emulsions, suspensions and polymer solutions in which there may be a slip between the fluid and the boundary (wang [25]). The applications of such study in technology can be found in the polishing of artificial heart valves and internal cavities (Mukhopadhyay [12]). In view of this,

Anderson [26] examined the slip-flow of a Newtonian fluid over a linearly stretching sheet, Das [21] investigated slip effects on heat and mass transfer in MHD micropolar fluid flow over an inclined plate with thermal radiation and chemical reaction. Devi *et al.* [27] examined radiation effect on MHD slip flow past a stretching sheet with variable viscosity and heat source/sink. Nandeppanavar *et al.* [28] investigated flow and heat transfer in MHD Newtonian fluid flow over a stretching sheet with variable thermal conductivity and partial slip.
The aim of this study is to investigate the flow, heat and mass transfer in MHD non-Newtonian micropolar fluid under the influence of thermal radiation, higher order chemical reaction, viscous dissipation, heat generation/absorption, with velocity and thermal slips over an exponentially stretching sheet with exponential temperature and concentration distributions. The nonlinear partial differential equations of the flow are transformed into nonlinear ordinary differential equations by an appropriate similarity transformations while the resulting equations are solved by applying the shooting method with fourth order Runge-Kutta integration scheme.

2 Problem Formulation

Consider a steady, two-dimensional, laminar boundary layer slip flow of a viscous, incompressible chemically reacting and electrically conducting micropolar fluid past an exponentially stretching sheet. The cartesian coordinate system is (x, y, z) and the corresponding velocity components are $(u, v, 0)$. The x-axis is directed towards the continuous stretching sheet along the flow while the y-axis is normal to it. The stretching velocity is assumed to be $u_w = U_0 e^{\frac{x}{L}}$ while the velocity upstream is assumed to be zero, the temperature and concentration of the sheet are $T_w = T_w = T_\infty + T_0 e^{\frac{x}{2L}}$ and $C_w = C_\infty + C_0 e^{\frac{x}{2L}}$ respectively. The flow is confined to the region $y > 0$. A transverse variable magnetic field $B(x)$ is applied normal to the flow direction as displayed in Fig. 1. Also, the angular velocity $\boldsymbol{\omega} = (\omega_1,\ \omega_2,\ \omega_3) = (0, 0, N(x, y))$ is assumed. The radiative heat flux term in x direction is considered negligible as compared to that in the y direction. It is assumed also that the magnetic Reynolds number is sufficiently small such that the induced magnetic field is negligible as compared to the applied magnetic field.

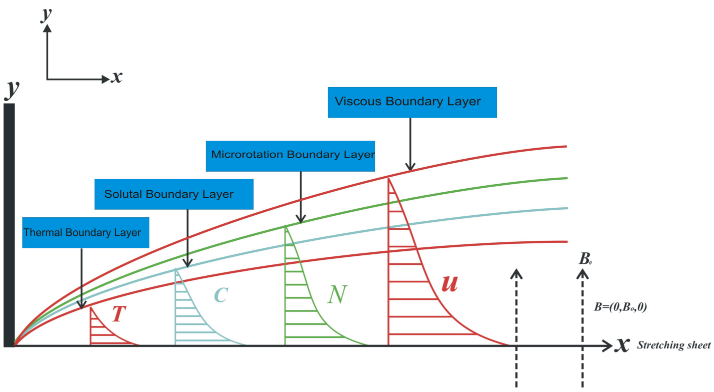

Fig. 1. Geometry of the flow.

Under the stated assumptions and the boundary layer approximations, the governing boundary layer continuity, momentum, microrotation, energy and concentration equations are respectively given as:

$$\frac{\partial u}{\partial x} + \frac{\partial v}{\partial y} = 0, \tag{1}$$

$$u\frac{\partial u}{\partial x} + v\frac{\partial v}{\partial y} = \frac{(\mu+\kappa)}{\rho}\frac{\partial^2 u}{\partial y^2} + \frac{\kappa}{\rho}\frac{\partial N}{\partial y} - \frac{\sigma B^2(x)}{\rho}u, \tag{2}$$

$$u\frac{\partial N}{\partial x} + v\frac{\partial N}{\partial y} = \frac{\gamma}{\rho j}\frac{\partial^2 N}{\partial y^2} - \frac{\kappa}{\rho j}\left(2N + \frac{\partial u}{\partial y}\right), \tag{3}$$

$$u\frac{\partial T}{\partial x}+v\frac{\partial T}{\partial y}=\frac{k}{\rho C_p}\frac{\partial^2 T}{\partial y^2}+\frac{\mu+\kappa}{\rho C_p}\left(\frac{\partial u}{\partial y}\right)^2-\frac{1}{\rho C_p}\frac{\partial q_r}{\partial y}+\frac{\sigma B^2(x)}{\rho C_p}u^2+\frac{Q_0}{\rho C_p}\left(T-T_\infty\right), \tag{4}$$

$$u\frac{\partial C}{\partial x}+v\frac{\partial C}{\partial y}=Dm\frac{\partial^2 C}{\partial y^2}-k_r\left(C-C_\infty\right)^n \tag{5}$$

The associated boundary conditions for Eqs. 1, 2, 3, 4 and 5 are:

$$\begin{aligned} &y=0:\ u=u_w+A\frac{\partial u}{\partial y},\ v=V_w\left(x\right),T=T_w+B\frac{\partial T}{\partial y},\ C=C_w,N=-m\frac{\partial u}{\partial y}\\ &y\longrightarrow\infty:\ u\longrightarrow 0,\ N\longrightarrow 0,\ T\longrightarrow\infty,\ C\longrightarrow\infty. \end{aligned} \tag{6}$$

Here $u_w=U_0e^{\frac{x}{L}}$ is the stretching velocity, $T_w=T_\infty+T_0e^{\frac{x}{2L}}$ is the sheet Temperature, U_0 is the reference velocity, T_0 is the reference temperature, $A=\alpha_1e^{\frac{-x}{2L}}$ is the velocity slip factor which changes with x, $B=\beta_1e^{\frac{-x}{2L}}$ is the thermal slip factor which changes with x (Mukhopadhyay [12]), the variable magnetic field $B(x)$ is assumed to be $B(x)=B_0e^{\frac{x}{2L}}$ (Seini and Makinde [17]), where B_0 is the constant magnetic field, positive and negative values of V_w indicates injection and suction respectively
Also, u and v are the velocity components in x and y directions respectively, ρ, κ, T, C, N, σ, C_p, q_r, Q_0, k_r and n are the fluid density, vortex viscosity, fluid temperature, fluid concentration, component of microrotation whose direction of rotation lies perpendicular to the $xy-$ plane, electrical conductivity, specific heat at constant pressure, radiative heat flux, heat source/sink, chemical reaction rate, and order of chemical reaction. Also, A is the velocity slip, B is the thermal slip, k is the thermal conductivity, Dm is the molecular diffusivity, j is the spin gradient viscosity and m is the boundary parameter with $0\leq m\leq 1$. The case $m=0$ corresponds to $N=0$, this represents no-spin condition i.e. strong concentration such that the micro-particles close to the wall are unable to rotate, $m=\frac{1}{2}$ indicates weak concentration of micro-particles and the vanishing of anti-symmetric part of the stress tensor and the case $m=1$ represents turbulent boundary layer flows (see Peddieson [29]; Ahmadi, [30]; Jena and Mathur [31]).
Using Rosseland approximation,

$$q_r=-\frac{4\sigma^\star}{3\alpha^\star}\frac{\partial T^4}{\partial \bar{y}} \tag{7}$$

is the radiative heat flux (Adeniyan [32]; Akinbobola and Okoya [33]), here $\sigma^\star$ is the Stefan-Boltzmann constant, $\alpha^\star$ is the mean absorption coefficient.
Assuming that there exists sufficiently small temperature difference within the flow such that T^4 can be expressed as a linear combination of the temperature. Expanding T^4 in Taylor series about T_∞ to get

$$T^4=T_\infty^4+4T_\infty^3\left(T-T_\infty\right)+6T_\infty^2\left(T-T_\infty\right)^2+..., \tag{8}$$

neglecting higher order terms in Eq. (8) gives

$$T^4=4T_\infty^3T-3T_\infty^4, \tag{9}$$

hence

$$\frac{\partial q_r}{\partial \bar{y}}=-\frac{16\sigma^\star T_\infty^3}{3\alpha^\star}\frac{\partial T^2}{\partial y^2}. \tag{10}$$

Following El-Aziz [15]; Seini and Makinde [17]), the following similarity transformations are introduced

$$\begin{aligned} &\eta=\left(\frac{U_0}{2L\nu}\right)^{\frac{1}{2}}e^{\frac{x}{2L}},\psi=\left(2\nu LU_0\right)^{\frac{1}{2}}e^{\frac{x}{2L}}f(\eta),\ u=U_0e^{\frac{x}{L}}f'(\eta),\ v=-\left(\frac{U_0\nu}{2L}\right)^{\frac{1}{2}}e^{\frac{x}{L}}\left(f(\eta)+\eta f'(\eta)\right)\\ &N=\left(\frac{U_0^3}{2L\nu}\right)^{\frac{1}{2}}e^{\frac{3x}{2L}},\ T=T_\infty+T_0e^{\frac{x}{2L}}\theta(\eta),\ C=C_\infty+C_0e^{\frac{x}{2L}}\phi(\eta), \end{aligned} \tag{11}$$

where η is the dimensionless similarity variable, ψ is the stream function defined as $u = \frac{\partial\psi}{\partial y}, v = -\frac{\partial\psi}{\partial x}$ which identically satisfies the mass conservation Eq. (1), $f(\eta)$ is the dimensionless stream function, $\theta(\eta)$ is the dimensionless temperature, $\phi(\eta)$ is the dimensionless concentration and prime denote differentiation with respect to η. Substituting Eq. (11) into (2-5) and using Eq. (8) in (4) yields the following non-linear ODEs:

$$(1+K)\,f''' + ff'' - 2f'^2 + Kg' - Mf' = 0 \tag{12}$$

$$\lambda g'' + fg' - 3f'g - 2H\left(2g + f''\right) = 0 \tag{13}$$

$$\left(1+\frac{4}{3}R\right)\theta'' + PrEc\,(1+K)\,f''^2 - Pr\left(f'\theta - f\theta'\right) + PrEcMf'^2 + PrQ\theta = 0 \tag{14}$$

$$\phi'' - Sc\left(f'\phi - f\phi'\right) - Sc\zeta\phi^n = 0 \tag{15}$$

subject to boundary conditions:

$$\begin{aligned} &\eta = 0 : f' = 1 + \alpha f'',\ f = fw,\ g = -mf'',\ \theta = 1 + \beta\theta', \phi = 1 \\ &\eta \longrightarrow \infty : f' = 0,\ g \longrightarrow 0,\ \theta \longrightarrow 0, \phi \longrightarrow 0 \end{aligned} \tag{16}$$

Here, prime denotes differentiation with respect to η, $K = \frac{\kappa}{\mu}$ is the material parameter, $\alpha = \alpha_1\sqrt{\frac{U_0}{2\nu L}}$ is the velocity slip parameter, $\alpha_1 = Ae^{-\frac{x}{2L}}$ is the initial value of the velocity slip factor, $\beta = \beta_1\sqrt{\frac{U_0}{2\nu L}}$ is the thermal slip parameter, $\beta_1 = Be^{-\frac{x}{2L}}$ is the initial value of the thermal slip factor [12], $Pr = \frac{\mu C_p}{k}$ is the Prandtl number, $R = \frac{4\sigma^\star T_\infty^3}{k\star k}$ is the radiation parameter, $M = \frac{2L\sigma B_0^2}{U_0\rho}$ is the magnetic field parameter, $fw = -\frac{V_w}{e^{\frac{x}{2L}}}\left(\frac{2L}{U_0\nu}\right)^{\frac{1}{2}}$ is the suction (>0)/injection (<0), $\lambda = \frac{\gamma}{\mu j}$ is the microrotation density parameter, $H = \frac{\kappa L}{\rho j U_0}$ is the vortex viscosity parameter, $Q = \frac{2L}{\rho C_p u_w}$ is the heat source/sink parameter, $Ec = \frac{u_w^2}{C_p(T_w - T_\infty)}e^{\frac{2x}{L}}$ is the Eckert number, $\zeta = \frac{2Lk_r(C_w - C_\infty)^{n-1}}{U_0}$ is reaction rate parameter and n is the order of chemical reaction.

The quantities of engineering interest are the local skin friction coefficient, the Nusselt number, the Sherwood number, the wall couple stress. Following El-Aziz [15], these are respectively defined as:

$$\begin{aligned} &C_{f_x} = \frac{1}{\rho u_w^2}\left[(\mu+\kappa)\frac{\partial u}{\partial y} + \kappa N\right]_{y=0},\quad Nu_x = \frac{L}{(T_w - T_\infty)}\left(-\frac{\partial T}{\partial y}\right)_{y=0} \\ &Sh_x = \frac{L}{(C_w - C_\infty)}\left(-\frac{\partial C}{\partial y}\right)_{y=0}, M_w = \left(\gamma\frac{\partial N}{\partial y}\right)_{y=0}, \end{aligned} \tag{17}$$

In dimensionless form the skin friction, Nusselt number, Sherwood number and wall couple stress correspondingly become

$$\begin{aligned} &\frac{1}{\sqrt{2}}(Re_x)^{\frac{1}{2}}C_{f_x} = (1 + (1 - mK))\,f''(0),\ \left(\frac{1}{2}Re_x\right)^{-\frac{1}{2}}Nu_x = -\theta'(0) \\ &\left(\frac{1}{2}Re_x\right)^{-\frac{1}{2}}Sh_x = -\phi'(0), (Re_x)^{-\frac{1}{2}}, M_w = \frac{\gamma u_w^2}{2\nu L}g'(0), \end{aligned} \tag{18}$$

where $Re_x = \frac{u_w x}{\nu}$ is the local Reynolds number

3 Method of Solution

The coupled nonlinear differential equations (12-15) with the boundary conditions (16) is a Boundary Value Problem (BVP) which are solved using shooting method alongside fourth order Runge-Kutta method. The higher order equations (12-15) of third order in f, and second order in g, θ and ϕ are reduced into a system of nine simultaneous equations of first order for nine unknowns. To solve this system, nine initial conditions are required while only five initial conditions are available. Thus, four initial conditions are needed which are not given in the problem, these are: $f''(0), g'(0)$, $\theta'(0)$ and $\phi'(0)$. However, the values of f', g, θ and ϕ are known as $\eta \longrightarrow \infty$. These four end conditions are used to produce the four unknown initial conditions (p_1, p_2, p_3, p_4) at $\eta = 0$ by using the shooting technique. To estimate the value of η_∞ we start with some initial guess value and solve the BVP equations (12-15) to get $f''(0), g'(0)$, $\theta'(0)$ and $\phi'(0)$. The procedure is repeated until two successive values of $f''(0), g''(0)$, $\theta'(0)$ $\phi'(0)$ differ only after desired significant digit signifying the limit of the boundary along η. The last value of η is chosen as appropriate for a particular set of governing parameters for the determination of the dimensionless velocity $f'(\eta)$, microrotation $g(\eta)$, temperature $\theta(\eta)$ and concentration $\phi(\eta)$ across the boundary layer. To reduce the higher order equations to a system of first order differential equations we let:

$$f_1 = f, f_2 = f', f_3 = f'', f_4 = g, f_5 = g', f_6 = \theta, f_7 = \theta', f_8 = \phi, f_9 = \phi' \tag{19}$$

$$f_3' = \frac{f_2^2 - f_1 f_3 - K f_5 + M f_2}{(1+K)}, \tag{20}$$

$$f_5' = \frac{3 f_2 f_4 + 2H\,(2 f_4 + f_3) - f_1 f_5}{\lambda}, \tag{21}$$

$$f_7' = \frac{Pr\left[(f_2 f_6 - f_1 f_7) - Ec\,(1+K)\, f_3^2 - EcM f_2 f_6 f_2^2 - Q f_6\right]}{\left(1 + \frac{4}{3}R\right)}, \tag{22}$$

$$f_9' = Sc\zeta f_8^n + Sc\,(f_2 f_8 f_1 f_9)\,. \tag{23}$$

The boundary conditions become

$$\begin{gathered} f_1(0) = f_w, f_2(0) = 1 + \alpha f_3(0), f_3(0) = p_1, f_4(0) = -n f_3(0), f_5(0) = p_2, f_6(0) = 1 + \beta f_7(0), \\ f_7(0) = p_3, f_8(0) = 1, f_9(0) = p_4, f_2(\infty) \longrightarrow 0, f_4(\infty) \longrightarrow 0, f_6(\infty) \longrightarrow 0, f_8(\infty) \longrightarrow 0 \end{gathered} \tag{24}$$

Thereafter, after gotten all the initial conditions, fourth-order Runge-Kutta integration scheme with step size $\nabla\eta = 0.05$ is applied and the solution is obtained with a tolerance limit of 10^{-7}. The computations are carried out by a program coded in a symbolic language Maple 18. From the numerical computation, the skin friction coefficient $f''(0)$, the Nusselt number $-\theta'(0)$, the wall couple stress $g'(0)$ and the Sherwood number $\phi'(0)$ are found and presented in Table 3.

4 Results and Discussion

To have clear insight into the behaviour of the fluid flow, a computational analysis has been carried out for the dimensionless velocity, temperature, concentration and microrotation for various values of the velocity slip parameter α, thermal slip parameter β, material (micropolar) parameter K, vortex viscosity parameter λ, radiation parameter R, chemical rate of reaction parameter ζ, order of chemical reaction parameter n, suction/injection parameter fw, heat generation parameter Q. The default values adopted for computation are: $K = \beta = \lambda = n = \zeta = M = 1$, $Pr = 0.72$, $R = Ec = 0.1$, $Q = -0.2$, $H = m = 0.5$ and $Sc = 0.62$. The graphs correspond to these values unless otherwise indicated.
In order to verify the accuracy of the numerical scheme used in this work, comparisons of the present results in respect to the values of the Nusselt number $-\theta'(0)$ have been made with the existing work of Bidin and Nazar [34], Ishak [35], Seini and Makinde [17] and Mukhopadhyay [12] for some limiting cases as shown in Table 1. The comparisons are found to be in good agreement.

Table 1: Values of $-\theta'(0)$ for variation in Pr and R compared to existing results when $\alpha = \beta = K = Sc = \zeta = m = M = H = fw = \lambda = Q = Ec = n = 0$

Pr	R	Bidin & Nazar [34]	Ishak [35]	Seini & Makinde [17]	Mukhopadhyay [12]	Present results
1.0	0.0	0.9547	0.9548	0.984811	0.9547	0.9548106
3.0	0.0	1.8691	1.8691	1.869060	1.8691	1.8690688
5.0	0.0		2.5001	2.500128	2.5001	2.5001280
10	0.0		3.6604	3.660369	3.6603	3.6603693
1.0	0.5	0.6765				0.6775462
1,0	1.0	0.5315	0.5312		0.5311	0.5353012
2.0	0.5	1.0735			1.0734	1.0735162
3.0	0.5	1.3807			1.3807	1.3807451

Table 2 depicts the values of the skin friction coefficient $f''(0)$ and heat transfer coefficient $-\theta'(0)$ for variation in radiation parameter R, magnetic field parameter M and Eckert number Ec as compared with that of [17] in the absence of the velocity slip parameter α, thermal slip parameter β, material (micropolar) parameter K and suction/injection parameter fw. The comparisons are found to be in good agreement

Table 2: Values of $f''(0)$ and $-\theta'(0)$ with [17] for variation in R, M and Ec when $Pr = 0.71, Sc = 0.24, \zeta = n = 1$ and $\alpha = \beta, K = H = m = 0$

			Seini & Makinde [17]		Present Results	
R	M	Ec	$-f''(0)$	$-\theta'(0)$	$-f''(0)$	$-\theta'(0)$
0.0	1.0	1.0	1.629178	0.006338	1.629178	0.006338
0.1	1.0	1.0	1.629178	0.006964	1.629178	0.006965
0.5	1.0	1.0	1.629178	0.035754	1.629178	0.459923
0.1	2.0	1.0	1.912620	-0.276418	1.912620	-0.276418
0.1	5.0	1.0	2.581130	-0.874464	2.581130	-0.874464
0.1	10.0	1.0	3.415289	-1.153452	3.415290	-1.536591
0.1	1.0	1.0	1.629178	0.006964	1.629178	0.006965
0.1	1.0	2.0	1.629178	-0.598521	1.629178	-0.598521
0.1	1.0	3.0	1.629178	-1.204006	1.629178	-1.204006

Table 3 displays the computational values of the skin friction coefficient, the local Nusselt number, the local Sherwood number and the wall couple stress for variation in the velocity parameter α, thermal slip parameter β, material parameter K, heat source/sink parameter Q, suction/injection parameter and chemical reaction parameter ζ. From this table, it is found that an increase in the velocity slip parameter α causes a reduction in the skin friction, Nusselt number, Sherwood number and the wall couple stress whereas an increase in fw has the exact opposite effect. Similarly, a rise the thermal slip parameter β decreases the Nusselt number while it has no effect on the skin friction coefficient, Sherwood number and the wall couple stress. A rise in the material parameter K leads to a decrease in both the skin friction and the wall couple stress while the opposite trend is observed for the heat and mass transfer rates. The rate of mass transfer also increases with an increase in the rate of chemical reaction ζ.

Table 3: Values of $-f''(0), -\theta'(0), -\phi'(0)$ and $-g'(0)$ for varying values of α, β, K, Q, fw and ζ

α	β	K	Q	fw	ζ	$-f''(0)$	$-\theta'(0)$	$-\phi'(0)$	$g'(0)$
0.0	1.0	1.0	-0.2	0.5	1.0	1.165924	0.466564	0.498763	1.025623
0.5						0.681269	0.454178	0.432430	0.496035
1.5						0.387813	0.432699	0.378757	0.233498
0.3	1.0					0.811615	0.888203	0.452322	0.628176
	2.0					0.811615	0.605753	0.452322	0.628176
	3.0					0.811615	0.370265	0.452322	0.628176
	1.0	0.0				1.130453	0.434659	0.891765	0.873466
		1.0				0.811615	0.459601	0.994994	0.628176
		2.0				0.664698	0.469187	1.047335	0.513730
		1.0	0.05			0.811615	0.417220	1.096904	0.628176
			0.15			0.811615	0.391803	1.096904	0.628176
			0.5			0.811615	0.311219	0.672770	0.325540
				-1.0		0.688525	0.356113	0.789315	0.401561
				-0.5		0.811615	0.459600	1.096904	0.628176
				0.5		0.881867	0.510266	1.286923	0.792278
				1.0	0.2	0.811615	0.459600	0.584242	0.628176
				0.5	1.0	0.811615	0.459600	0.758253	0.628176
					0.5	0.811615	0.459600	0.883001	0.628176

Figs. 2-3 depict the influence of magnetic field parameter M on the velocity and temperature profiles. Evidently, the velocity decreases with an increase in the value of the magnetic field parameter M. This response is due to the imposition of the transverse magnetic field in an electrically conducting fluid which induces a drag-like force known as Lorentz force which act against the fluid motion and slows it down. However, the temperature rises with increasing values of M as displayed in Fig. 3.

Figs. 4-7 illustrate the influence of the material parameter K on the velocity, temperature, microrotation and concentration profiles. It is evident that the velocity profile increases with an increase in K due to the increase in the hydrodynamic boundary layer thickness as shown in Fig. 4. On the other hand, the temperature, concentration and the microrotation profiles decrease as K increases. The decrease in the microrotation profile however, is only near the exponentially stretcing sheet, further from the sheet, the profile overlap and then increase as displayed in Fig. 6.

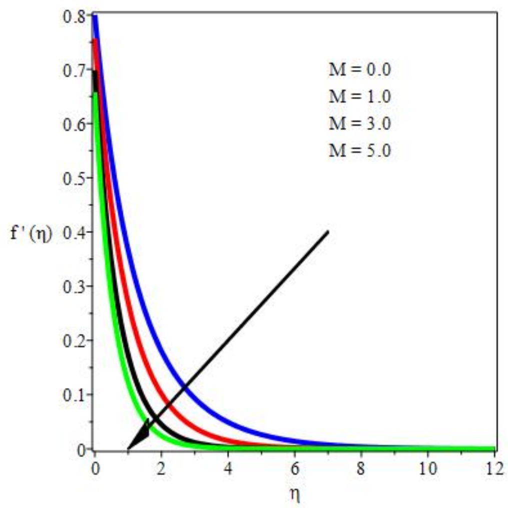

Fig. 2. Effect of M on velocity profiles

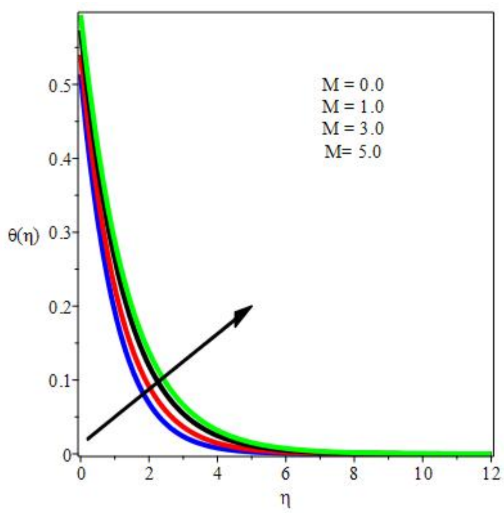

Fig. 3. Effect of M on temperature profiles

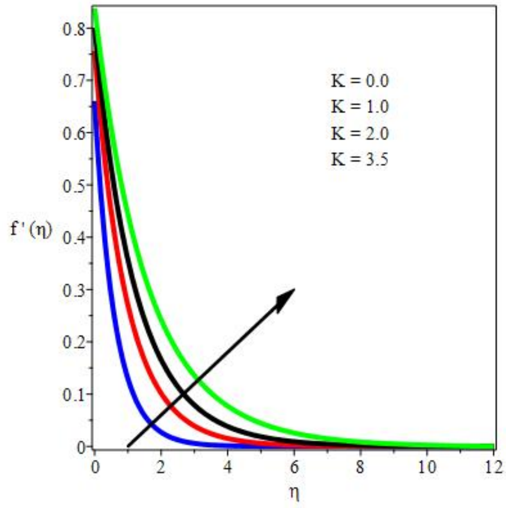

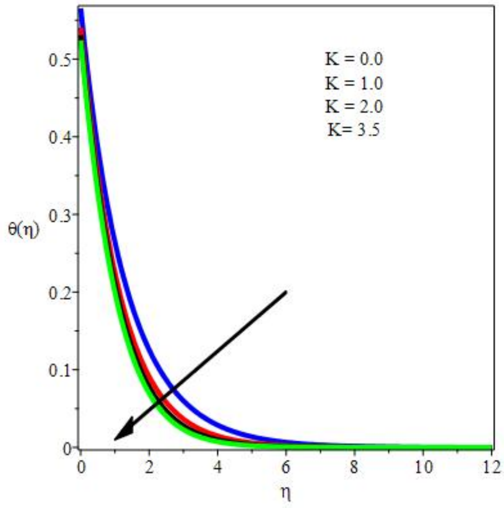

Fig. 4. Effect of K velocity profiles **Fig. 5.** Effect of K on Temperature

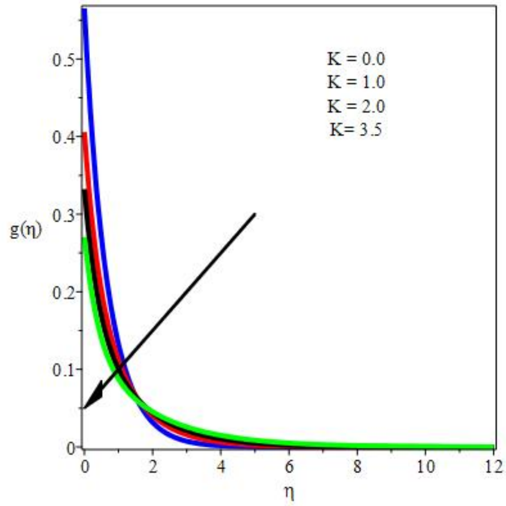

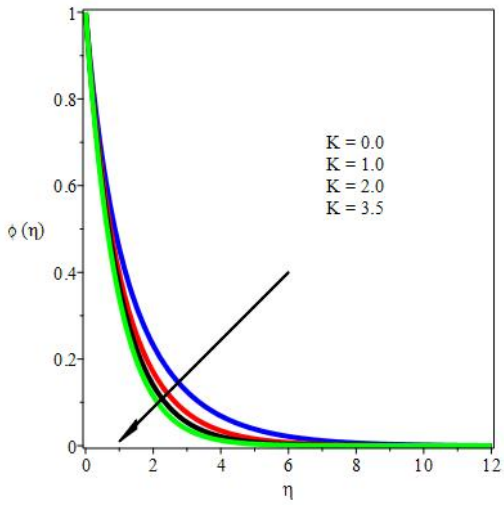

Fig. 6. Effect of K on Microrotation profiles **Fig. 7.** Effect of K on concentration

Figs. 8-9 describe the effects of the velocity slip parameter α on the velocity and temperature profiles across the boundary layer. There is a reduction in the fluid velocity as α increases as shown in Fig. 8. Moreover, it is noticed that the rate of transport reduces with the increasing distance (η) from the sheet for the velocity profiles. In the presence of slip, the stretching velocity and the flow velocity near the sheet are unequal. Therefore, an increase in the slip parameter α causes a rise in the slip velocity leading to a decrease in the fluid velocity as observed in Fig. 8. Meanwhile, an increase in α enhances the temperature distribution due to the thickening of the thermal boundary layer thickness as shown in Fig. 9.

Fig. 10 shows that an increase in the thermal slip parameter β causes a decrease in temperature profiles. This response is due to the fact that as β increases, less heat is transferred from the sheet to the fluid leading to a drop in the temperature. (see Table 3). Figs. 11-13 describe the influence of the suction/injection parameter fw on the velocity, temperature and concentration profiles. A decrease in the velocity, temperature and microrotation profiles is observed with an increase in the suction parameter (fw). An increase in $fw > 0$ causes a thinning effects on these profiles due to the fact that the heated fluid is being pushed towards the sheet such that the fluid is brought closer to the surface leading reduction in the, momentum, thermal and solutal boundary layer thicknesses. However, the imposition of wall fluid injection $fw < 0$ produces the opposite effect as it enhances velocity, thermal and solutal distribution within the boundary layer.

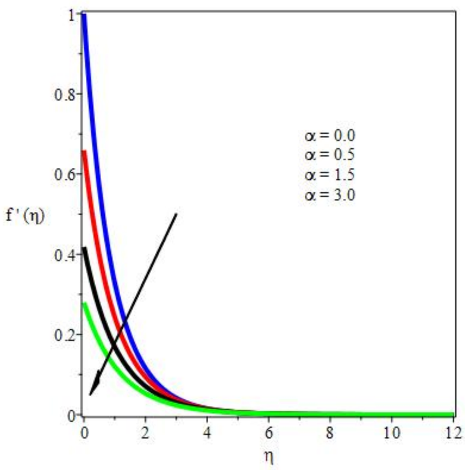

Fig. 8. Effect of α on Velocity profiles

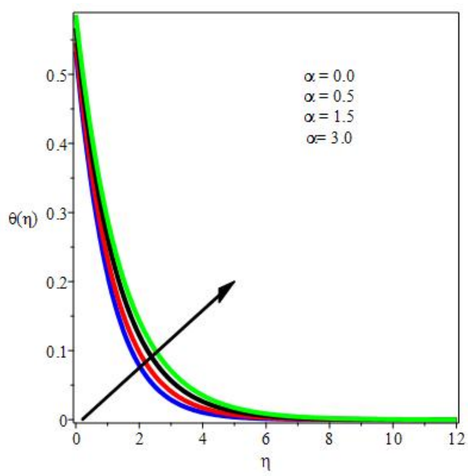

Fig. 9. Effect of α on Temperature

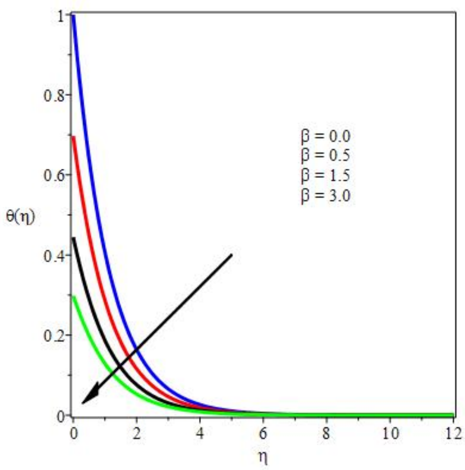

Fig. 10. Effect of β on Temperature profiles

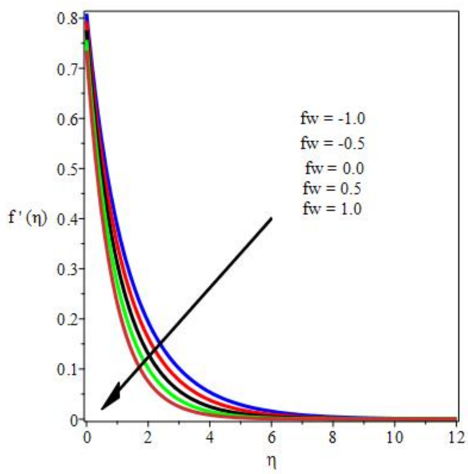

Fig. 11. Effect of fw on Velocity

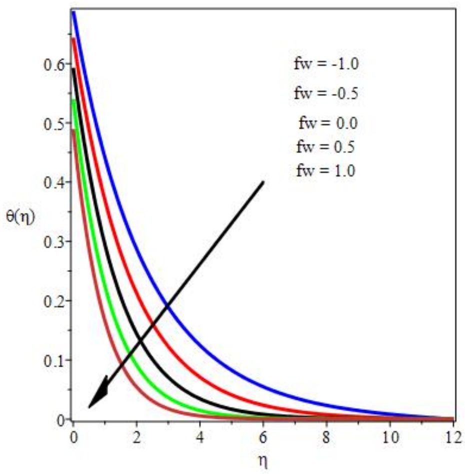

Fig. 12. Effect of fw on Temperature profiles

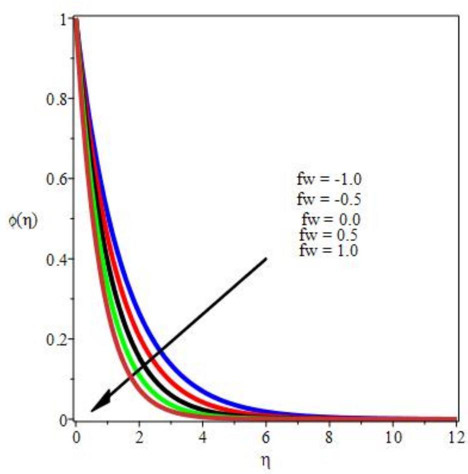

Fig. 13. Effect of fw on Concentration profiles

Fig. 14 describes the variation of temperature profiles with η for different values of Eckert number Ec. Observation shows that increasing values of Ec enhances temperature distribution and the thermal boundary layer thickness. This response is due the fact that as Ec increases, heat is generated as a result of the drag between the fluid particles, the internal heat generation inside the fluid increases the bulk fluid temperature which is an indication of additional heating in the flow region due to viscous dissipation, thus, the additional heat causes increase in the fluid temperature. The effect of radiation parameter R on the temperature distribution is displayed in Figure 15. Evidently, the temperature profile increases as the magnitude of R increases. This is due to the fact that the divergence of the radiative heat flux increases as the Rosseland mean absorption coefficient decreases. Thus, the rate of radiative heat transfer to the fluid rises and then causing the temperature of the fluid to rise. Hence, the cooling process is at a faster rate if R reduced.

Fig. 18 depicts the influence of the homogeneous chemical reaction rate parameter ζ on the concentration profiles. An increase in ζ causes a decrease in the concentration of the micropolar fluid flow along the exponentially stretching sheet due to the thinning of the solutal boundary layer thickness. In contrast, an increase in the order of the chemical reaction n enhances the concentration profiles as shown in Fig. 17. The influence of heat generation parameter Q on the dimensionless temperature profile is illustrated in Fig. 18. Clearly, an increase in Q enhances the temperature distribution due to a rise in the thermal boundary layer thickness as Q increases. In addition, energy is generated by the imposition $Q > 0$ leading to an increase in the micropolar fluid temperature, thereby causing a rise in the temperature profiles. Fig. 19 describes the effect of the microrotation density parameter λ on the microrotation profile. It is noticed that the microrotation profile rises with an increase in λ due to a rise in the microrotation boundary layer thickness.

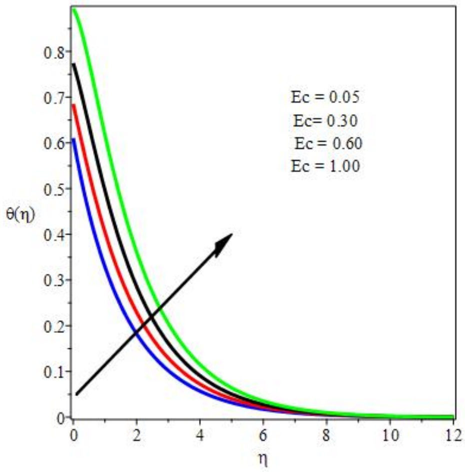

Fig.14. Effect of Ec on Temperature

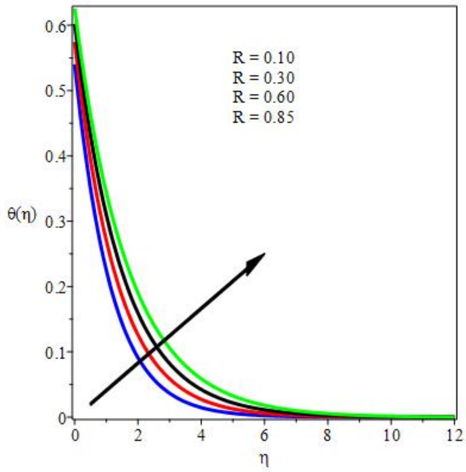

Fig.15. Effect of R on Temperature

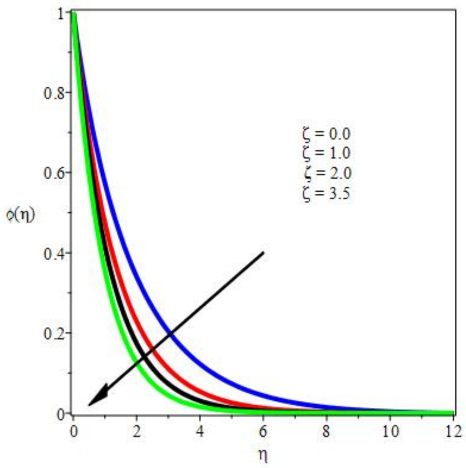

Fig. 16. Effect of ζ on Concentration

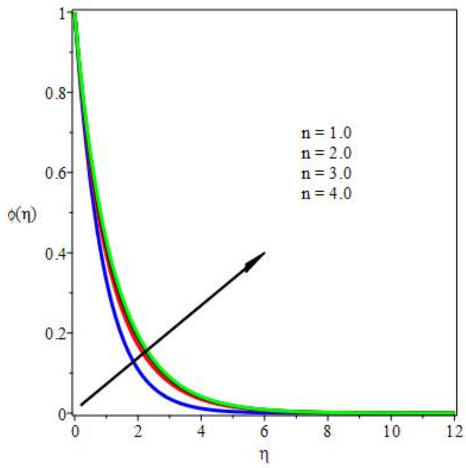

Fig. 17. Effect of n on Concentration

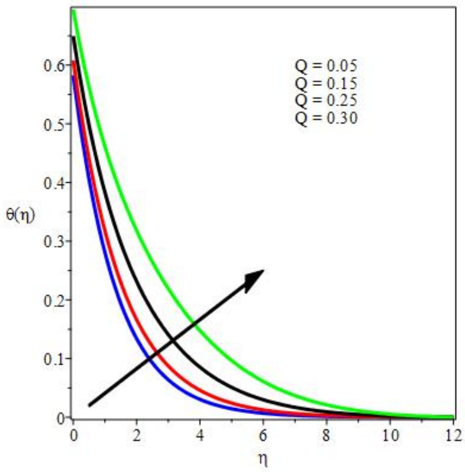

Fig. 18. Effect of Q on Temperature

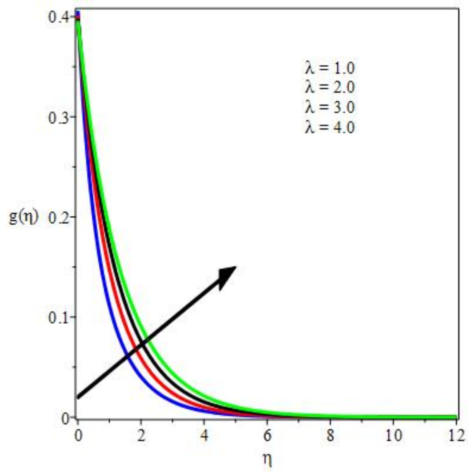

Fig. 19. Effect of λ on Microrotation

Conclusion

The problem of hydromagnetic micropolar fluid flow, heat and mass transfer over an exponentially stretching sheet under the influence of thermal radiation, viscous dissipation, surface mass flux, chemical reaction and slip effects has been investigated. The resulting equations governing the fluid flow are solved by shooting method alongside Runge-Kutta integration technique. The results compared well with the existing result in the literature in some limiting cases and the influences of the emerging physical parameters on the dimensionless velocity, microrotation, temperature and species concentration profiles as well as on the skin friction coefficient $f''(0)$, wall couple stress $g'(0)$, Nusselt number $-\theta'(0)$ and the Sherwood number $-\phi'(0)$ are presented through graphs and tables. The following conclusions are drawn from this study:

- The material (micropolar) parameter K causes a reduction in the skin friction coefficient $f''(0)$ and the wall couple stress $g'(0)$ whereas the rate of heat transfer $-\theta'(0)$ and mass transfer $-\phi'(0)$ rise with an increase in K. Thus, the material parameter K can be useful in reducing drag along the stretching sheet while it increases the rate of heat transfer.

- An increase in the velocity slip parameter α also reduces the skin friction coefficient $f''(0)$ as the thermal slip parameter β reduces the rate of heat transfer.

- An increase in the order of the chemical reaction enhances the concentration profiles as the rate of mass transfer is enhanced by the chemical reaction rate. However, the rate of the chemical reaction causes a decrease in the species concentration of the micropolar fluid flow.

- The thermal radiation, heat generation and viscous dissipation enhance the temperature profiles and the thermal boundary layer thickness while the trend is reversed with the imposition of suction.

References

[1] Eringen, A. C. Theory of micropolar fluids, *J. Math. Anal. Appl.*, 1966; **16**, 1-18.
[2] Eringen, A. C. Theory of thermo-microfluids, *Journal of Mathematical Analysis and Applications*, 1972; **38**, 480-496.
[3] Chen, J., Liang, C. and Lee J. D. Theory and simulation of micropolar fluid dynamics, *J.Nanoengineering and nanosystems*, 2011; **224**, 31-39.
[4] Hayat, T., Shehzad, S. A. and Qasim, M. Mixed convection flow of a micropolar fluid with radiation and chemical reaction, *Int J. Numer Meth*, 2011; 67, 1418-1436.
[5] Lukaszewicz, G. *Micropolar fluids: Theory and Applications* 1st Ed., Birkhauser, Boston, 1999.
[6] Peddieson, J and McNitt, R. P. Boundary layer theory for micropolar fluid, *Recent Adv. Enggng Sci.*, **5**, 405 (1970).
[7] Crane, L. J. Flow past a stretching plate, *Communicatios Breves*, 1970; **21**, 645-647.

[8] Gupta, P. S. and Gupta, A. S. Heat and mass transfer on a stretching sheet with suction or blowing, *Can. J. Chem. Eng.*, 1977; **55**, 744-746.

[9] Eldabe, N. T., Elshehawey, E. F., Elbarbary, M. E. and Elgazery, N. S. Chebyshev finite difference method for MHD flow of a micropolar fluid past a stretching sheet with heat transfer, *Journal of Applied Mathematics and Computation*, 2003; **160**, 437-450.

[10] Elbashbeshy, E. M. A. and Bazid, M. A. A. Heat transfer in a porous medium over a stretching surface with internal heat generation and suction or injection *Applied Mathematics and Computation*, 2004; **158**, 799-807.

[11] Reddy, M. G. Heat generation and thermal radiation effects over a stretching sheet in a micro polar fluid, *Int. Scholarly Research Network*, 2012; **2012**, 1-6.

[12] Mukhopadhyay, S. Slip effects on MHD boundary layer flow over an exponentially stretching sheet with suction/blowing and thermal radiation, *Ain Shams Engineering Journal*, 2013; **2013**, 485-491.

[13] Magyari, E & Keller, B. Heat and mass transfer in the boundary layers on an exponentially stretching continuous surface *Journal of Physics*, 1999; **32**, 577-585.

[14] Sajid, M and Hayat, T. Influence of thermal radiation on thermal radiation on the boundary layer flow due to exponentially stretching sheet, *International Communication in Heat and Mass Transfer*, 2008; **35**, 347-356.

[15] El-Aziz, M. Viscous dissipation effect on mixed convection flow of a micropolar fluid over an exponentially stretching sheet, *can. J. Phy*, 2009; **87**, 359-368.

[16] Mandal, I. and Mukhopadhyay, S. Heat transfer analysis for fluid flow over an exponentially stretching porous sheet with surface heat flux, *Ain Shams Eng. Journal*, 2013; **2013**, 103-110.

[17] Seini, Y. I. and Makinde, O. D. MHD boundary layer flow due to exponentially stretching surface with radiation and chemical reaction *Mathematical Problem in Engineering*, 2013; **2013**, 1-7.

[18] Kumar, L. Finite element analysis of combined heat and mass transfer in hydromagnetic micro polar flow along a stretching sheet. *Comput Mater Sci*(2009); **46**, 841-848.

[19] Ibrahim, S. M. Effects of chemical reaction on dissipative radiative MHD flow through a porous medium over a nonisothermal stretching sheet, *Journal of Industrial Mathematics, Research*, 2014; **2014**, 1-10 (2010).

[20] Hamad, M. A. A., Uddin, M. J, and Ismail, A. I. Radiation effects on heat and mass transfer in MHD stagnation-point flow over a permeable flat plate with thermal convective surface boundary condition, temperature dependent viscosity and thermal conductivity, *Nuclear Engineering and Design*, 2012; **242**, 194-200.

[21] Das, K. Slip effects on heat and mass transfer in MHD microplar fluid flow over an inclined plate with thermal radiation and chemical reaction, *Int. J. Numer. Meth. Fluids*, 2012; Doi:10.2002/fd.2683.

[22] Mishra, S .R, Baag, S. and Mohapatra, D. K. Chemical reaction and Soret effects on hydro magnetic micropolar fluid along a stretching sheet, *Engineering Science and Technology, an Inter national Journal*, **19**, **2016**; 1919-1928.

[23] Olajuwon, B. I, Oahimire, J. I and Waheed, W. A. Convection heat and mass transfer in a hydro magnetic flow of a micropolar fluid over a porous medium, *Theoret. Appl. Mech.*, 2014; **41**, 93-117.

[24] Pal, D. and Chatterjee, S. Heat and mass transfer in MHD non-Darcian flow of a micropolar fluid over a stretching sheet embedded in a porous media with non-uniform heat source and thermal radiation, *Commun Nonlinear Sci. Numer Simulat*, 2011; **15**, 1843-1857.

[25] Wang, C. Y. Flow due t o stretching boundary with partial slip- an exact solution of the Navier Stokes equation, *Chen Eng. Sci.*, 2002l; 57, 3745-3747.

[26] Anderson, H. I. Sip flow past a stretching surfcade, *Acta Mechanica*, (2002); **158**, 121-125.

[27] Devi, R. L., Neeraja, A. and Reddy, N. B. Radiation effect on MHD slip flow past a stretching sheet with variable viscosity and heat source/sink, *Int. J.Sci and Innovative Mathematical Res*, 2015; **3**, 8-17.

[28 Nandeppanavar, M. M., Vajravelu, K., Abel, M. S and Siddalingappa, M. N. MHD flow and heat transfer over a stretching surface with variable thermal conductivity and partial slip, *Meccanica*, 2013, **48**, 1451-1464.

[29] Peddieson, J. An application of the micropolar model to the calculation of a turbulent shear flow, *Int. J. Eng. Sci.*, 1972; 10, 23-32.

[30] Ahmadi, G. (1976). Self-similar solution of incompressible micropolar boundary layer flow over a semi-infinite plate, Int. J. Engng Sci, **14**, 639-646.

[31] Jena, S. K. & Mathur, M. N. Similarity solutions for laminar free convection flow of a thermo micropolar fluid past a non-isothermal flat plate, *International J. Eng. Sci.*, 1981; **19**, 1431-1439.

[32] Brewster, M. Q. *Thermal Radiative Transfer Properties*, Wiley, New York, NY, USA (1992).

[33] Akinbobola, T. E. & Okoya, S. S. The flow of second grade fluid over a stretching sheet with variable thermal conductivity and viscosity in the presence of heat source/sink, *Journal of Nigeria Mathematical Society*, 2015; **34**, 331-342.

[34] Bidin, B & Nazar, R. Numerical solution of the boundary layer over an exponentially stretching sheet, *European Journal of Scientific Research*, 2009; **33**, 710-717.

[35] Ishak, A. MHD boundary layer flow due to exponentially stretching sheet with radiation effect, *Sains Malayansian*, 2011; **40**, 391-395.